Joint Power System State Estimation and Breaker Status Identification

Vassilis Kekatos and Georgios B. Giannakis
Dept. of ECE, University of Minnesota
Minneapolis, MN 55455, USA
Emails:{kekatos,georgios}@umn.edu

***Abstract*—The penetration of renewables and demand-response programs will inevitably lead to frequent flow reversals and substation reconfigurations, while high-throughput synchrophasor measurement units are being installed throughout the grid. Hence, jointly verifying circuit breaker statuses and estimating the state of power networks of increasing dimensionality becomes even more challenging. Building on generalized state estimation, revisited in the light of modern measurement capabilities, the aforementioned task is relaxed to a convex optimization problem. Exploiting compressive sampling advances, the prior information on unmonitored and suspected switches takes the form of ℓ_2-norm penalties promoting sparsity in a properly defined block manner. An efficient algorithm is developed to ensure compatibility with solvers found currently at control centers. Numerical tests on the IEEE 14-bus model corroborate the effectiveness of the novel scheme.**

***Index Terms*—Alternating direction method of multipliers; generalized state estimator; intelligent electronic devices; phasor measurement units.**

I. Introduction

Topology processing and state estimation are two basic modules in power system monitoring [16]. When run separately, it is easily understood that even though topology errors can be detected through unacceptable state estimation outcomes, they are not easily identifiable by the state estimator [1, Ch. 8]. Merging the two modules under the so called generalized state estimation (GSE) task has been a well-appreciated solution [16].

By employing the bus section/switch instead of the bus/branch network model, GSE essentially estimates the system state augmented by circuit breaker flows. Open (closed) switching devices correspond then to zero flows (voltage drops). To ensure observability of the expanded model, breakers of known status are imposed as structural constraints [16]. But practically, not all circuit breakers are monitored; and even for the monitored ones, the reported status may be erroneous due to switch malfunctioning, communication failures, or manipulation by maintenance teams [1].

Detection of substation configuration errors has been considered in [11], [21], and [7]. The even challenging problem of identifying circuit breaker statuses is usually treated under the GSE framework. Least-absolute value (LAV) state estimators have been proposed in [17], [2]. The largest normalized residual test is borrowed from bad data detection and applied in [6] on the Lagrange multipliers corresponding to circuit breaker constraints. The robust Huber's M-estimator has been also considered in [15], while a probabilistic breaker status modeling is suggested in [13]. To handle the increased dimensionality of the network model involved in GSE, an equivalent reduced-size model has been developed in [8]. Jointly estimating the state and the faults in DC electric circuits via ℓ_1-norm regularization has been proposed in [10], and standard quadratic program solvers have been employed. Finally, [5] poses a mixed integer nonlinear program whose complexity is not deterministically polynomial.

Changes taking place in today's grids pose new challenges for GSE. The introduction of renewables and demand-response programs will eventually lead to frequent substation reconfigurations. The situational awareness vision calls for more accurate models, while the deregulated energy markets lead to even larger reliability footprints. On the other hand, technological advances in instrumentation should be leveraged [9]: phasor measurement units (PMU) able to record high-throughput voltage and current phasors invade the grids. Automation has reached even at the substation level, where intelligent electronic devices (IED) can provide important data to the control center too.

In this work, GSE is revisited under this new paradigm. Given phasor measurements, GSE for exact AC power system models can be posed as a linearly-constrained least-squares (LS) problem (Section II). Since only a limited number of circuit breakers can be reliably monitored, the bus section/switch model is likely to be unobservable. Prior information on the status of unmonitored breakers can potentially restore system identifiability. By leveraging compressive sampling advances, the GSE cost is regularized by ℓ_2-norms of selected vectors, which promote block sparsity on real/imaginary pairs (Section III). A computationally efficient solver is subsequently derived in Section IV. It operates on a reduced-size vector and is compatible with existing estimators installed at control centers. Numerical tests on an expanded version of the IEEE 14-bus power network show that the novel method can correct multiple breaker errors at the expense of a tolerable increase in complexity (Section V). The paper is concluded in Sec. VI. Regarding notation, lower- (upper-) case boldface letters de-

Dr. Kekatos is supported by a Marie Curie International Outgoing Fellowship within the 7-th European Community Framework Programme (No. 234914). This work was also supported by NSF grants CCF-1016605 and ECCS-1002180. Dr. Kekatos is also with the Computer Engnr. & Informatics Dept., University of Patras, Greece.

note column vectors (matrices); calligraphic letters stand for sets; and $(\cdot)^T$ denotes transposition.

II. System Modeling & Problem Statement

Consider the typical power system model at the bus section/switching device network level [1, Ch. 8], [16], consisting of N_b bus sections, henceforth called simply buses, N_l transmission lines, and N_s circuit breakers (switches). Let vectors $\tilde{\mathbf{v}} \in \mathbb{C}^{N_b}$ and $\tilde{\mathbf{i}}_l \in \mathbb{C}^{2N_l}$ contain the bus voltages and the electric currents injected at both sides of every transmission line, respectively. If $\tilde{\mathbf{Y}}_l$ is the associated line-bus admittance matrix, Kirchoff's and Ohm's laws imply

$$\tilde{\mathbf{i}}_l = \tilde{\mathbf{Y}}_l \tilde{\mathbf{v}}. \tag{1}$$

To model the effect of switching devices, consider the circuit breaker current vector $\tilde{\mathbf{s}} \in \mathbb{C}^{N_s}$ where current directionality is conventionally assumed from lower- to higher-indexed buses. Define also the $N_s \times N_b$ switch-bus incidence matrix $\mathbf{A}$ whose i-th row $\mathbf{a}_i^T$ corresponding to the (m, n) switch between buses m and n with $m < n$ has its m-th (n-th) entry equal to $+1(-1)$, and zero elsewhere. When the (m, n) switch is open, no current flows on it $\tilde{s}_i = 0$. When it is closed, the voltage difference between its ends is zero, i.e., $\mathbf{a}_i^T \tilde{\mathbf{v}} = \tilde{v}_m - \tilde{v}_n = 0$.

The bus current injection vector can be expressed as

$$\tilde{\mathbf{i}} = \tilde{\mathbf{Y}} \tilde{\mathbf{v}} + \mathbf{A}^T \tilde{\mathbf{s}} \tag{2}$$

where $\tilde{\mathbf{Y}} \in \mathbb{C}^{N_b \times N_b}$ is the bus admittance matrix.

Power systems are currently being instrumented with contemporary metering devices, such as phasor measurement units (PMU) and intelligent electronic devices (IED); see e.g., [9]. Once a PMU is installed on a bus, it can potentially measure its voltage and injection current together with the current phasors from all the lines incident to that bus. IEDs can record the current flowing on a subset of circuit breakers and report the status of others. Assuming that PMU and IED measurements are available at the control center, the problem considered here is that of jointly estimating the underlying system state and determining the status of unmonitored circuit breakers.

To concretely formulate the problem, it is useful to review the notion of generalized state estimation (GSE), and explicitly model the cost function as well as the structural and operational constraints involved; see e.g., [1, Ch. 8], [16]. In GSE, the power system state is augmented from the vector $\tilde{\mathbf{v}}$ to include the breaker current vector $\tilde{\mathbf{s}}$ too. Specifically, the vector of system states in rectangular coordinates is expressed as $\mathbf{x}^T := \left[\mathbf{v}^T \ \mathbf{s}^T\right]$ and is of dimension $N := 2(N_b + N_s)$, where $\mathbf{v}^T := \left[\mathrm{Re}\{\tilde{\mathbf{v}}^T\} \ \mathrm{Im}\{\tilde{\mathbf{v}}^T\}\right]$ and $\mathbf{s}^T := \left[\mathrm{Re}\{\tilde{\mathbf{s}}^T\} \ \mathrm{Im}\{\tilde{\mathbf{s}}^T\}\right]$.

To model the analog readings collected at the control center, four types of measurements should be identified first: (M1) nodal voltages; (M2) current injections; (M3) line current flows; and (M4) circuit breaker flows. If all M measurements are expressed in rectangular coordinates too, the following linear model is obtained

$$\mathbf{z} = \mathbf{H}_v \mathbf{v} + \mathbf{H}_s \mathbf{s} + \mathbf{e} = \mathbf{H}\mathbf{x} + \mathbf{e} \tag{3}$$

where $\mathbf{H}_v$ and $\mathbf{H}_s$ will be defined soon, $\mathbf{H} := [\mathbf{H}_v \ \mathbf{H}_s] \in \mathbb{R}^{M \times N}$, and the vector $\mathbf{e}$ captures instrumentation errors and modeling inaccuracies. The latter is modeled as a random vector of zero mean and known covariance matrix. Since measurements can be easily pre-whitened, the noise covariance matrix can be modeled as the identity matrix without loss of generality. The rows of $\mathbf{H}_v$ and $\mathbf{H}_s$ corresponding to (M1) measurements are simply the appropriate rows of the identity matrix and the zero vectors, respectively. The converse holds for (M4) measurements. For (M2) and (M3) measurements, the related rows can be obtained after expressing (2) and (1) in rectangular coordinates, respectively.

The linear model of (3) supposes availability of synchrophasor measurement units. Note however, that conventional SCADA measurements, i.e., (re)active nodal power injections and line power flows together with bus voltage magnitudes, do not adhere to a linear model. Actually, performing state estimation using those types of measurements entails solving non-convex optimization problems. Typically, such models are iteratively linearized using the Gauss-Newton method. Then, (3) corresponds to the postulated model per Gauss-Newton iteration. The same holds even when SCADA and PMU measurements are jointly considered.

Using the bus section/switch network model increases the number of states, and thus, the risk of loosing system observability. Any prior information and breaker statuses should be taken into account as well in the form of constraints as described next. Three types of constraints are typically encountered in GSE: (C1) zero-injection buses; (C2) open circuit breakers; and (C3) closed circuit breaker constraints. All the three constraints are modeled next.

Let $\mathcal{N}$ denote the set of null-injection buses. Based on (2), the (C1) constraints can be expressed as

$$\mathbf{Y}_{\mathcal{N}} \mathbf{v} + \mathbf{A}_{\mathcal{N}}^T \mathbf{s} = \mathbf{0} \tag{4}$$

where

$$\mathbf{Y} := \begin{bmatrix} \mathrm{Re}\{\tilde{\mathbf{Y}}\} & -\mathrm{Im}\{\tilde{\mathbf{Y}}\} \\ \mathrm{Im}\{\tilde{\mathbf{Y}}\} & \mathrm{Re}\{\tilde{\mathbf{Y}}\} \end{bmatrix} \tag{5}$$

while $\mathbf{Y}_{\mathcal{N}}$ and $\mathbf{A}_{\mathcal{N}}^T$ are the submatrices obtained after retaining only the rows of $\mathbf{Y}$ and $\mathbf{A}^T$, respectively, corresponding to the null injection buses. Conformably, if $\mathcal{O}$ and $\mathcal{C}$ are the sets of circuit breakers whose status is reliably reported to the control center, constraints (C2) and (C3) can be written as

$$\mathbf{s}_{\mathcal{O}} = \mathbf{0} \tag{6}$$

$$\mathbf{A}_{\mathcal{C}} \mathbf{v} = \mathbf{0}. \tag{7}$$

Based on the previous modeling, the least-squares estimate (LSE) of the augmented system state can be obtained as

$$\hat{\mathbf{x}}_{\mathrm{LSE}} := \arg\min_{\mathbf{x}} \quad \frac{1}{2}\|\mathbf{z} - \mathbf{H}\mathbf{x}\|_2^2 \tag{8a}$$

$$\text{s.t.} \quad \mathbf{C}\mathbf{x} = \mathbf{0} \tag{8b}$$

where the single constraint in (8b) expresses collectively the constraints (C1)-(C3), and matrix $\mathbf{C}$ has size $C \times N$, where

$C := 2 \cdot (|\mathcal{N}| + |\mathcal{O}| + |\mathcal{C}|)$. The linearly-constrained convex quadratic program of (8) can be solved in closed form.

The solution of (8) is unique, provided the measurement and constraint sets are sufficiently large and dense so that the augmented state is observable. However, even if the system is observable, the state estimates in $\hat{\mathbf{x}}_{\text{LSE}}$ related to uninstrumented breakers will be generally erroneous in the following sense: neither currents flowing on open uninstrumented breakers will be zero, nor the voltage drops across closed uninstrumented breakers will be. To alleviate these issues, this work suggests exploiting any further breaker information available at the control center in the manner described next.

III. Proposed Method

One should recall that the control center has historical data on typical substation configuration patterns that could be used as prior information for unknown-status circuit breakers. Additionally, there exist circuit breakers that even though their status is recorded, that information has been deemed unreliable, e.g., by preliminary (local) topological results, possible manipulation by maintenance team working nearby, or large residuals. Due to these two reasons, the status of such breakers, henceforth collected in set $\mathcal{S}$, is mostly speculative and unreliable. It cannot be used as a hard constraint (C2)-(C3) in (8), but rather it has to be verified.

More concretely, consider the 2×1 vector comprising the real and imaginary currents flowing on the supposedly open m-th circuit breaker, i.e., $[\text{Re}\{\tilde{s}_m\}\ \ \text{Im}\{\tilde{s}_m\}]^T$ which can be written as $\mathbf{S}_m\mathbf{x}$ for an appropriately defined $2 \times N$ selection matrix. Similarly, consider the vector of real and imaginary voltage drops across the assumingly closed n-th breaker, that is $[\mathbf{a}_m^T \operatorname{Re}\{\tilde{\mathbf{v}}\}\ \ \mathbf{a}_m^T \operatorname{Im}\{\tilde{\mathbf{v}}\}]^T$, which can also be expressed as $\mathbf{S}_n\mathbf{x}$.

Since all the suspected breakers would satisfy their expected status, all the $\mathbf{S}_m\mathbf{x}$ vectors for $m \in \mathcal{S}$ will be most likely zero. Hence, to jointly estimate the system state and identify the breaker statuses in $\mathcal{S}$, one could solve a variation of the LSE in (8) where the cost function is penalized by the number of breakers in $\mathcal{S}$ not satisfying their expected outcomes. This can be formulated as

$$\min_{\mathbf{x}} \quad \frac{1}{2}\|\mathbf{z} - \mathbf{H}\mathbf{x}\|_2^2 + \lambda_0 \sum_{m \in \mathcal{S}} \operatorname{I}(\|\mathbf{S}_m\mathbf{x}\|_2) \quad \text{s.t.} \quad \mathbf{C}\mathbf{x} = \mathbf{0} \tag{9}$$

where $\operatorname{I}(|x|)$ is equal to one when $|x| > 0$, and zero otherwise. The penalty parameter λ_0 indicates the confidence to the prior information: when $\lambda_0 = 0$, the problem in (9) reduces to the original problem of (8), which means that prior information on unmonitored breakers is ignored and detecting the statuses relies solely on state estimation. On the other hand, for $\lambda_0 \to \infty$, all breakers in $\mathcal{S}$ are set to their expected status, and prior information becomes indisputable.

Solving (9) is combinatorially complex. Nevertheless, spurred by advances in the compressive sampling literature [4], it can be relaxed to a convex optimization problem. Under certain conditions on the involved problem parameters ($\mathbf{H}$, $\mathbf{C}$, $\{\mathbf{S}_m\}$), the relaxed problem solution coincides or is close in the ℓ_1- or ℓ_2-norm sense to the hard problem solution. The indicator function $\operatorname{I}(|x|)$ in (9) can be relaxed to $|x|$, which is the closest convex approximation of the former when $|x| \leq 1$. Hence, the $\operatorname{I}(\|\mathbf{S}_m\mathbf{x}\|_2)$ summands in the cost of (9) are replaced by $\|\mathbf{S}_m\mathbf{x}\|_2$.

Upon this surrogation, the convex relaxation of (9) is then

$$\min_{\mathbf{x}} \quad \frac{1}{2}\|\mathbf{z} - \mathbf{H}\mathbf{x}\|_2^2 + \lambda \sum_{m \in \mathcal{S}} \|\mathbf{S}_m\mathbf{x}\|_2 \quad \text{s.t.} \quad \mathbf{C}\mathbf{x} = \mathbf{0} \tag{10}$$

which can be essentially solved as a second-order cone program (SOCP). Interestingly, compressive sampling offers assurance that due to the ℓ_2-norm penalties in the cost, the minimizers of (10) will have most of their $\{\mathbf{S}_m\mathbf{x}\}_{m \in \mathcal{S}}$ terms set to zero as a whole; see e.g., [22], [18], [12]. Two points should be stressed. First, having many of the $\{\mathbf{S}_m\mathbf{x}\}_{m \in \mathcal{S}}$ vectors with both entries equal to zero is the desiderata here. In other words, problem (10) promotes *block sparsity* as opposed to single-entry sparsity pursued by [10]. Second, it is exactly the non-squared ℓ_2-norm penalties that promote this form of sparsity.

IV. An Efficient Algorithm

Problem (10) can be solved by standard interior point-based solvers. However, such second-order solvers may not be adequate for handling a real-world power system consisting of some thousands of buses, each modeled by 1-10 bus sections and connected to 2-3 transmission lines. More importantly, such solvers are incompatible with the currently available power system state estimation software.

To tackle these issues, an efficient algorithm for solving (10) is developed here. It is based on the alternating direction method of multipliers (ADMM), a method that has been successfully applied for several optimization tasks; see [3] for a review.

Firstly, aiming to convert (10) to an equivalent unconstrained problem, observe that the equality constraint in (10) implies that there exists a vector $\mathbf{u}$ such that the minimizer $\mathbf{x}$ satisfies $\mathbf{x} = \mathbf{B}\mathbf{u}$, where the columns of matrix $\mathbf{B} \in \mathbb{R}^{N \times (N-C)}$ span the null space of $\mathbf{C}$. Then, solving (10) is equivalent to solving

$$\min_{\mathbf{u}} \quad \frac{1}{2}\|\mathbf{z} - \bar{\mathbf{H}}\mathbf{u}\|_2^2 + \lambda \sum_{m \in \mathcal{S}} \|\bar{\mathbf{S}}_m\mathbf{u}\|_2 \tag{11}$$

with $\bar{\mathbf{H}} := \mathbf{H}\mathbf{B}$ and $\bar{\mathbf{S}}_m := \mathbf{S}_m\mathbf{B}$ for $m = 1, \ldots, S$.

Next, let us introduce the auxiliary optimization variable $\mathbf{w} \in \mathbb{R}^{2S}$, and rewrite (11) as

$$\min_{\mathbf{u},\mathbf{w}} \quad \frac{1}{2}\|\mathbf{z} - \bar{\mathbf{H}}\mathbf{u}\|_2^2 + \lambda \sum_{m \in \mathcal{S}} \|\mathbf{w}_m\|_2 \tag{12a}$$

$$\text{s.t.} \quad \bar{\mathbf{S}}\mathbf{u} = \mathbf{w} \tag{12b}$$

where $\bar{\mathbf{S}}$ contains matrices $\{\bar{\mathbf{S}}_m\}$ stacked vertically as $\bar{\mathbf{S}}^T := [\bar{\mathbf{S}}_1^T\ \bar{\mathbf{S}}_2^T \cdots \bar{\mathbf{S}}_S^T]$, and $\mathbf{w}$ has been conformably split to $\mathbf{w}_m$'s.

Adding this extra variable may seem redundant, but it facilitates the efficient solution of (12) as detailed next.

In general, ADMM exploits the method of multipliers (a.k.a. quadratic penalty method) concatenated with an iteration of the Gauss-Seidel algorithm. Specifically, for the problem in (12), let $\boldsymbol{\mu}$ be the Lagrange multiplier vector corresponding to the constraint (12b). The augmented Lagrangian function is

$$L(\mathbf{u}, \mathbf{w}; \boldsymbol{\mu}) := \frac{1}{2}\|\mathbf{z} - \bar{\mathbf{H}}\mathbf{u}\|_2^2 + \lambda \sum_{m \in \mathcal{S}} \|\mathbf{w}_m\|_2 + \boldsymbol{\mu}^T \left(\bar{\mathbf{S}}\mathbf{u} - \mathbf{w}\right) + \frac{c}{2}\|\bar{\mathbf{S}}\mathbf{u} - \mathbf{w}\|_2^2 \tag{13}$$

where c is a positive constant. Letting r denote the iteration index, ADMM cycles through three steps:

$$\mathbf{u}^{r+1} := \arg\min_{\mathbf{u}} L\left(\mathbf{u}, \mathbf{w}^r; \boldsymbol{\mu}^r\right) \tag{14a}$$

$$\mathbf{w}^{r+1} := \arg\min_{\mathbf{w}} L\left(\mathbf{u}^{r+1}, \mathbf{w}; \boldsymbol{\mu}^r\right) \tag{14b}$$

$$\boldsymbol{\mu}^{r+1} = \boldsymbol{\mu}^r + c\left(\bar{\mathbf{S}}\mathbf{u}^{r+1} - \mathbf{w}^{r+1}\right). \tag{14c}$$

At step (14a), $\mathbf{u}$ is updated by minimizing the augmented Lagrangian function while keeping the other (primal and dual) variables fixed to their previous iteration values. Likewise, $\mathbf{w}$ is updated in (14b). Finally, (14c) is a gradient ascent of $L\left(\mathbf{u}^{r+1}, \mathbf{w}^{r+1}; \boldsymbol{\mu}\right)$ with step size c.

The focus next is on implementing these three steps efficiently. Step (14c) entails a simple matrix-vector multiplication, while a minimizer of (14a) can be obtained as

$$\mathbf{u}^{r+1} = \left(c \cdot \bar{\mathbf{S}}^T\bar{\mathbf{S}} + \bar{\mathbf{H}}^T\bar{\mathbf{H}}\right)^{\dagger} \left(\bar{\mathbf{H}}^T\mathbf{z} + \bar{\mathbf{S}}^T\left(c\mathbf{w}^r - \boldsymbol{\mu}^r\right)\right) \tag{15}$$

where $(\cdot)^{\dagger}$ denotes matrix pseudoinverse. It is shown next how step (14b) involving the minimization

$$\min_{\mathbf{w}} \; \lambda \sum_{m \in \mathcal{S}} \|\mathbf{w}_m\|_2 - \left(\boldsymbol{\mu}^r\right)^T \mathbf{w} + \frac{c}{2}\|\bar{\mathbf{S}}\mathbf{u}^{r+1} - \mathbf{w}\|_2^2 \tag{16}$$

can be easily solved. Interestingly, the cost in (16) decouples nicely over the $\mathbf{w}_m$'s as

$$\min_{\mathbf{w}_m} \; \lambda\|\mathbf{w}_m\|_2 - \left(\boldsymbol{\mu}_m^r\right)^T \mathbf{w}_m + \frac{c}{2}\|\bar{\mathbf{S}}_m\mathbf{u}^{r+1} - \mathbf{w}_m\|_2^2 \tag{17}$$

where $\boldsymbol{\mu}^r$ has been split into $\boldsymbol{\mu}_m^r$'s conformably to the partition of $\mathbf{w}$. Using the subdifferential of the cost in (17), it can be shown that the minimizer is provided by the simple formula (see e.g., [12, Sec. V.B])

$$\mathbf{w}_m^{r+1} = \frac{1}{c} \cdot \mathbf{d}_m^r \left[1 - \frac{\lambda}{\|\mathbf{d}_m^r\|_2}\right]_+ \tag{18}$$

where $[x]_+ := \max\{x, 0\}$ and $\mathbf{d}_m^r := \boldsymbol{\mu}_m^r + c \cdot \bar{\mathbf{S}}_m\mathbf{u}^{r+1}$. In a nutshell, the update rule of (18) first calculates vector $\mathbf{d}_m^r$. If its ℓ_2-norm is larger than λ, then $\mathbf{w}_m^{r+1}$ is updated to $\mathbf{d}_m^r$ scaled by $(1 - \lambda/\|\mathbf{d}_m^r\|_2)/c$; otherwise, $\mathbf{w}_m^{r+1}$ is set to zero.

The proposed scheme is tabulated as Algorithm 1. It is worth mentioning that the algorithm does not require any special optimization solver, but it can be implemented by power system state estimation software already installed at the control centers.

Algorithm 1 Novel Algorithm

Require: Matrices $\mathbf{H}$, $\mathbf{S}$, $\mathbf{C}$; and positive parameters c, λ.

Find matrix $\mathbf{B}$ whose columns span the null space of $\mathbf{C}$.
Calculate $\bar{\mathbf{H}} := \mathbf{HB}$ and $\bar{\mathbf{S}} := \mathbf{HS}$.
Initialize $\mathbf{u}^0$, $\mathbf{w}^0$, $\boldsymbol{\mu}^0$ to zero.
for $r = 1, 2, \ldots$ **do**
  Update $\mathbf{u}^{r+1}$ via (15).
  Update $\mathbf{w}_m^{r+1}$ using (18) for $m = 1, \ldots, S$.
  Update $\boldsymbol{\mu}^{r+1}$ via (14c).
end for
Output $\mathbf{x} = \mathbf{Bu}$ for the final $\mathbf{u}$.

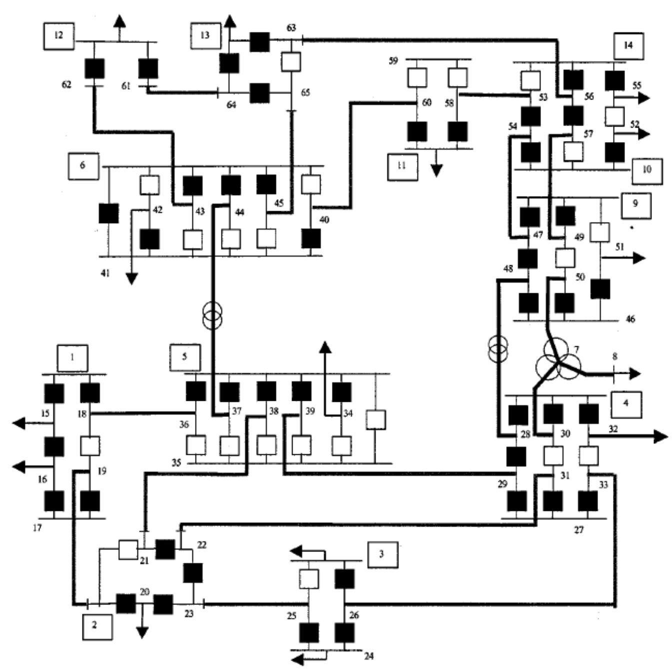

Fig. 1. The IEEE 14-bus power system modeled at the substation level [8]. Solid (hollow) squares indicate circuit breakers whose actual status is closed (open). The original 14 buses preserve their numbering. Thick lines correspond to finite-impedance transmission lines, and thinner ones to zero-impedance circuit breaker connections.

V. Simulated Tests

In this section, the novel joint state estimation and breaker status identification approach is numerically tested using the IEEE 14-bus power network [20]. The admittance matrix of the network and the underlying power system state are obtained using the MATPOWER software [23]. The IEEE 14-bus benchmark has been modeled at the substation level following the expansion of [8] as shown in Fig. 1. The buses of the original bus/branch model have been expanded to groups of bus sections following typical substation configurations (single bus, double bus/double breaker, main and transfer bus, breaker and a half, ring bus).

The state vector contains the real and imaginary parts of all bus voltages and circuit breaker currents. The measurements include PMU and IED recordings on voltage and current phasors expressed in rectangular coordinates too. Measurement noise is simulated as independent zero Gaussian with standard deviation per real component $\sigma_V = 0.01$ and $\sigma_I = 0.02$, for voltages and currents, respectively [23]. The different measurement types are detailed next. Among all the 65 buses, bus voltages measurements are collected at the 30 buses indicated by either boxed numbers, the bus-bar symbol, or the injection symbol; e.g., buses 1, 17, and 15, respectively. Electric currents are recorded at the 15 injection buses. Current phasor meters are assumed on both sides of all the 20 transmission lines. Finally, IEDs are assumed to record the current flow on all 73 logical circuit breakers. Hence, the measurement set comprises 316 real-valued recordings.

All the 50 bus sections not marked with the injection symbol are assumed to be null-injection buses, hence yielding a total of 100 structural constraints. Concerning the status of circuit breakers, they are divided into two main sets: breakers which are assumed either open or closed and are contained in set $\mathcal{S}$, and the remaining breakers with known status belonging to subsets $\mathcal{O}$ and $\mathcal{C}$ providing additional operational constraints.

A. Effectiveness

The new approach's capability to jointly estimate the power system state and identify the status of circuit breakers is justified through the following simulation setup. Subsets of breakers $\mathcal{S}$ with unreported status are sampled uniformly at random from $\{1, \ldots, 73\}$. In 80% of the breakers in $\mathcal{S}$, the assumed status coincides with the actual one, and is reversed for the rest 20%. The cardinality of $\mathcal{S}$ varies from 10 to 70 breakers.

The block sparsity-aware approach of Section II is compared to an ordinary generalized state estimator. The latter corresponds to simply solving (10) for $\lambda = 0$. For both methods, after the system state has been estimated, the statuses of the breakers in $\mathcal{S}$ are determined via the corresponding circuit current states. Two performance metrics are considered: the mean-square error (MSE) of the state estimates and the number of breaker status identification errors. Justified by numerical tests, the penalty parameter λ is equal to $1,000$ for all experiments.

The number of breaker status errors obtained by the two methods for sets $\mathcal{S}$ of increasing cardinality is plotted in Fig. 2. The conventional GSE cannot identify the unreported circuit breaker statuses. On the contrary, the proposed approach can partially correct the status of breakers in $\mathbf{S}$ while simultaneously estimating the augmented state. Figures 3 and 4 show the MSEs on the original 14 bus voltages and the full augmented state, respectively. The MSE curves indicate that misidentified breaker statuses deteriorate state estimation accuracy too, even at the higher bus/branch network model.

B. Computational Aspects

Having checked the effectiveness of the method, its computational aspects are numerically evaluated next. Numerical simulations using the previously described simulation setup has been run on an Intel Duo Core @ 2.2 GHz (4GB RAM) computer using MATLAB. The novel approach entails

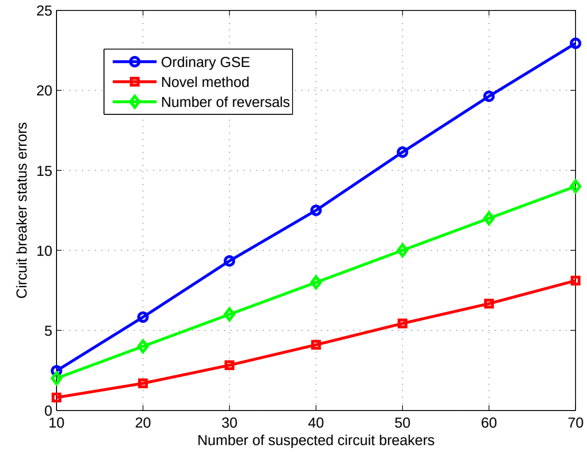

Fig. 2. Circuit breaker identification errors for sets $\mathcal{S}$ of increasing cardinality.

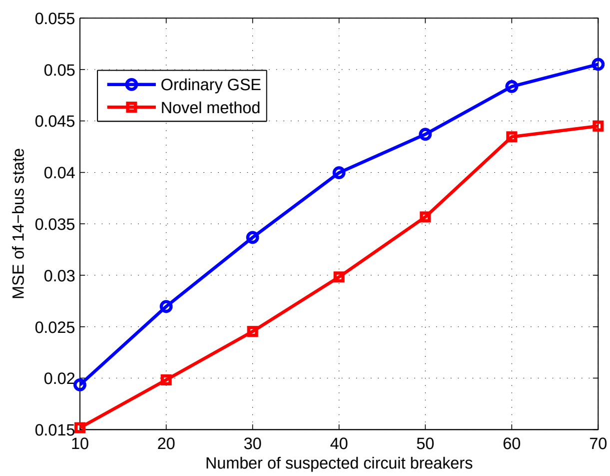

Fig. 3. MSE of substation voltages (original 14 buses) for sets $\mathcal{S}$ of increasing cardinality.

solving the unconstrained problem in (11) to obtain $\mathbf{u}$ and subsequently finding the system state as $\mathbf{x} = \mathbf{B}\mathbf{u}$. Regarding the first computationally demanding step, the problem in (11) is solved either as an SOCP using interior point-based standard solvers (SDPT3 [19] and [14]), or by using the steps of Alg. 1. For a fair comparison to GSE, the first step of the GSE is implemented by calculating the closed-form solution of (11) for $\lambda = 0$, i.e., $\mathbf{x}_{\text{GSE}} = \bar{\mathbf{H}}\mathbf{z}$.

For a meaningful computational comparison, the Lagrangian penalty parameter c should be tuned first. Numerical tests performed under various simulation setups showed that the convergence time of Alg. 1 remains basically invariant for a value of $c = 10^4$, which was fixed for all the succeeding tests. Then, the iterations needed from Alg. 1 to converge increase from 100 to 750 with increasing $|\mathcal{S}|$.

The computational time for the ordinary GSE and the proposed method solved using the standard solver and the derived algorithm is plotted in Fig. 5. The time needed by

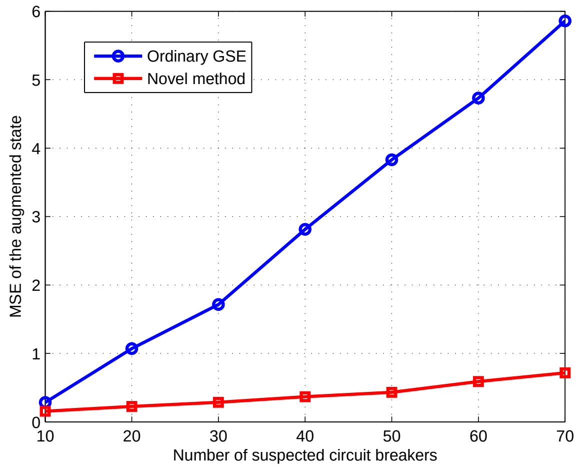

Fig. 4. MSE of the full (augmented) system state for sets $\mathcal{S}$ of increasing cardinality.

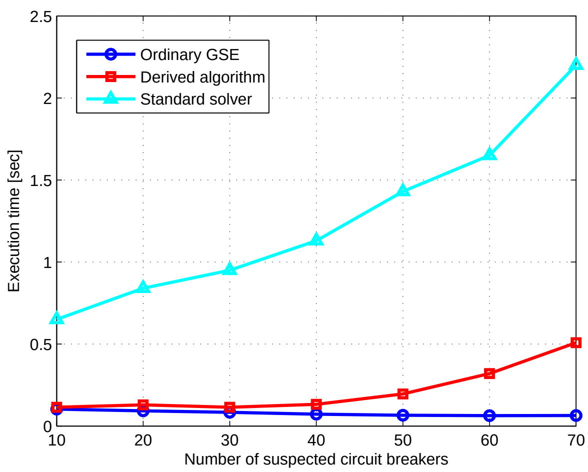

Fig. 5. Computational time of algorithms.

the ordinary GSE is slightly decreasing with increasing $|\mathcal{S}|$. The computational time of the derived algorithm is only 3-4 times higher than that of the GSE, even though it jointly estimates the states and reveals breaker status errors. Finally, the time complexity for the interior point-based solver scales unfavorably with the number of ℓ_2-norm penalties in the cost.

VI. Conclusions

A novel joint state estimation and circuit breaker identification method was introduced in this paper. The ordinary GSE was first reviewed to accommodate the linear measurement models and constraints offered by modern measurement units. Leveraging compressive sampling premises, the GSE cost was regularized by ℓ_2-norms of selected vectors to account for prior information on breakers of unknown status. Incorporating branch status errors and bad data measurements is the next interesting extension. To efficiently solve the optimization problem thus obtained, an ADMM-based algorithm was developed by operating on a transformed reduced-length vector state and consisting of simple updates. Numerical tests on the IEEE 14-bus model verified the effectiveness of the novel approach and the algorithm's efficiency. Studying the proposed scheme for practical power network dimensions is currently under investigation.

References

[1] A. Abur and A. Gomez-Exposito, *Power System State Estimation: Theory and Implementation*. New York, NY: Marcel Dekker, 2004.
[2] A. Abur, H. Kim, and M. Celik, "Identifying the unknown circuit breaker statuses in power networks," *IEEE Trans. Power Syst.*, vol. 10, no. 4, pp. 2029–2035, Nov. 1995.
[3] S. Boyd, N. Parikh, E. Chu, B. Peleato, and J. Eckstein, "Distributed optimization and statistical learning via the alternating direction method of multipliers," *Found. Trends Mach Learning*, vol. 3, pp. 1–122, 2010.
[4] E. J. Candes and T. Tao, "Decoding by linear programming," *IEEE Trans. Inf. Theory*, vol. 51, no. 12, pp. 4203–4215, Dec. 2005.
[5] E. Caro, A. Conejo, and A. Abur, "Breaker status identification," *IEEE Trans. Power Syst.*, vol. 25, no. 2, pp. 694–702, May 2010.
[6] K. A. Clements and A. S. Costa, "Topology error identification using normalized Lagrange multipliers," *IEEE Trans. Power Syst.*, vol. 13, no. 2, pp. 347–353, May 1998.
[7] A. S. Costa and J. A. Leao, "Identification of topology errors in power system state estimation," *IEEE Trans. Power Syst.*, vol. 8, no. 4, pp. 1531–1538, Nov. 1993.
[8] A. Gomez-Exposito and A. de la Villa-Jaen, "Reduced substation models for generalized state estimation," *IEEE Trans. Power Syst.*, vol. 16, no. 4, pp. 839–846, Nov. 2001.
[9] A. Gómez-Exposito, A. Abur, A. de la Villa Jaén, and C. Gomez-Quiles, "A multilevel state estimation paradigm for smart grids," *Proc. IEEE*, vol. 99, no. 6, pp. 952–976, Jun. 2011.
[10] D. Gorinevsky, S. Boyd, and S. Poll, "Estimation of faults in DC electrical power system," in *Proc. IEEE Conf. on Decision and Control*, Dec. 2009, pp. 4334–4339.
[11] M. R. Irving and M. J. Sterling, "Substation data validation," *Proc. Inst. Elect. Eng. C*, vol. 129, pp. 119–122, May 1982.
[12] V. Kekatos and G. B. Giannakis, "From sparse signals to sparse residuals for robust sensing," *IEEE Trans. Signal Process.*, vol. 59, no. 7, pp. 3355–3368, Jul. 2011.
[13] G. N. Korres and P. J. Katsikas, "Identification of circuit breaker statuses in WLS state estimator," *IEEE Trans. Power Syst.*, vol. 17, no. 3, pp. 818–825, Aug. 2002.
[14] J. Lofberg, "A toolbox for modeling and optimization in MATLAB," in *Proc. of the CACSD Conf.*, 2004. [Online]. Available: http://users.isy.liu.se/johanl/yalmip/
[15] L. Mili, G. Steeno, F. Dobraca, and D. French, "A robust estimation method for topology error identification," *IEEE Trans. Power Syst.*, vol. 14, no. 4, pp. 1469–1476, Nov. 1999.
[16] A. Monticelli, "Electric power system state estimation," *Proc. IEEE*, vol. 88, no. 2, pp. 262–282, Feb. 2000.
[17] H. Singh and F. L. Alvarado, "Network topology determination using least absolute value state estimation," *IEEE Trans. Power Syst.*, vol. 10, no. 3, pp. 1159–1165, Aug. 1995.
[18] M. Stojnic, F. Parvaresh, and B. Hassibi, "On the reconstruction of block-sparse signals with an optimal number of measurements," *IEEE Trans. Signal Process.*, vol. 57, no. 8, pp. 3075–3085, Aug. 2009.
[19] R. H. Tutuncu, K. C. Toh, and M. Todd, "Solving semidefinite-quadratic-linear programs using SDPT3," *Mathematical Programming Ser. B*, vol. 95, pp. 189–217, 2003.
[20] Power systems test case archive. University of Washington. [Online]. Available: http://www.ee.washington.edu/research/pstca/
[21] F. F. Wu and W. H. Liu, "Detection of topological errors by state estimation," *IEEE Trans. Power Syst.*, vol. 4, pp. 176–183, Feb. 1989.
[22] M. Yuan and Y. Lin, "Model selection and estimation in regression with grouped variables," *Journal of the Royal Statistical Society, Series B.*, vol. 68, no. 1, pp. 49–67, 2006.
[23] R. D. Zimmerman, C. E. Murillo-Sanchez, and R. J. Thomas, "MATPOWER: steady-state operations, planning and analysis tools for power systems research and education," *IEEE Trans. Power Syst.*, vol. 26, no. 1, pp. 12–19, Feb. 2011.